Pharmaceutical Research, Vol. 24, No. 6, June 2007 (© 2007)
DOI: 10.1007/s11095-007-9234-3

Research Paper

Effect of Solid Lipid Nanoparticles Formulation Compositions on Their Size, Zeta Potential and Potential for *In Vitro* pHIS-HIV-Hugag Transfection

Rathapon Asasutjarit,[1] Sven-Iver Lorenzen,[2] Sunee Sirivichayakul,[2] Kiat Ruxrungtham,[2] Uracha Ruktanonchai,[3] and Garnpimol C. Ritthidej[1,4]

Received October 7, 2006; accepted January 2, 2007; published online March 24, 2007

Purpose. This work was conducted to determine model equations describing the effect of solid lipid nanoparticles (SLN) formulation compositions on their size and zeta potential using the face-centered central composite design and to determine the effect of SLN formulation compositions on the potential for *in vitro* pHIS-HIV-hugag transfection.

Materials and Methods. SLN were prepared by the hot high pressure homogenization technique using cetylpalmitate as lipid matrix at varying concentrations of Tween 80 and Span 85 mixture, dimethyldioctadecyl ammonium bromide (DDAB) and cholesterol. Size and zeta potential used as responses of the design were measured at pH 7.0. The model equations were accepted as statistical significance at p value of less than 0.05. Ability of SLN to form complex with pHIS-HIV-hugag was evaluated by electrophoretic mobility shift assay. *In vitro* cytotoxicity of SLN was studied in HeLa cells using alamar blue bioassay. The potential of SLN for *in vitro* pHIS-HIV-hugag transfection was also determined in HeLa cells by western blot technique.

Results. SLN possessed diameter in a range of 136–191 nm and zeta potential 11–61 mV depending on the concentrations of surfactant mixture, DDAB and cholesterol. The regression analysis showed that the model equations of responses fitted well with quadratic equations. The ability of SLN to form complex with pHIS-HIV-hugag was also affected by formulation compositions. *In vitro* cytotoxicity results demonstrated that HeLa cells were not well tolerant of high concentrations of SLN but still survived in a range of 100–200 μg/ml of SLN in culture medium. The results of transfection study showed ability of SLN to use as a vector for *in vitro* pHIS-HIV-hugag transfection. However, their potential for *in vitro* transfection was lower than the established transfection reagent.

Conclusions. Size and zeta potential of SLN could be predicted from their quadratic model equations achieved by combination of three variables surfactant, DDAB and cholesterol concentrations. In addition, these variables also affected the potential of SLN as a vector for *in vitro* pHIS-HIV-hugag transfection. The results here provide the framework for further study involving the SLN formulation design for DNA delivery.

KEY WORDS: face-centered central composite design; HIV plasmid DNA vaccine delivery; size; solid lipid nanoparticles; zeta potential.

[1] Faculty of Pharmaceutical Sciences, Chulalongkorn University, Bangkok, 10330 Thailand.
[2] Faculty of Medicine, Chulalongkorn University, Bangkok, 10330 Thailand.
[3] National Nanotechnology Center, National Science and Technology Development Agency (NSTDA), Thailand Science Park, Pathumthani, 12120 Thailand.
[4] To whom correspondence should be addressed. (e-mail: rgarnpim@chula.ac.th)

ABBREVIATIONS: Adj. R^2, adjusted coefficient of determination; cm, centimeter; CO_2, carbon dioxide; CPC, cetylpyridinium chloride; CTAB, cetyltrimethylammonium bromide; -C, degree Celsius; DDAB, dimethyl dioctadecyl ammonium bromide; DMEM, Dulbecco's modified eagle's medium; DOTAP, N-[1-(2,3-dioleoyloxy)propyl]-N,N,N-trimethylammonium chloride; EDTA, ethylenediaminetetraacetic acid; EQ1, esterquat 1 (N,N-di-(B-stearoylethyl)-N,N-dimethyl-ammonium chloride; FBS, fetal bovine serum; g, gram; HAART, highly active antiretroviral therapy; HIV, human immunodeficiency virus; ml, milliliter; mV, millivolt; nm, nanometer; PBS, phosphate buffer saline; PCS, photon correlation spectroscopy; pDNA, plasmid deoxy ribonucleic acid; PI, polydispersity index; psi, pound per square inch; rpm, round per minute; SD, standard deviation; SLN, solid lipid nanoparticles; TAE, tris-acetate EDTA; TEM, transmission electron microscopy; UV, ultraviolet; v/v, volume by volume; w/v, weight by volume; w/w, weight by weight; μg, microgram; μl, microliter; %, percent.

INTRODUCTION

Development of biotechnology has led to the discovery of powerful DNA that can be employed for hereditary disorder improvement, life threatening diseases treatment such as cancer, infectious diseases and vaccination in healthy people to protect them from serious infectious diseases (1). However, DNA delivery is always restricted by poor stability of DNA in biological environment and limited transport across epithelia causing insufficient bioavailability. Therefore, an appropriate DNA delivery system should be to protect them from biological environments and facilitate transportation through biological barriers.

Solid lipid nanoparticles (SLN) have been recently proposed as an alternative carrier for DNA delivery (2). This is due to many technological advantages over other existing transfection vectors including production from generally recognized as safe substances, good storage stability and possibility of steam sterilization and lyophilization. In addition, SLN large-scale production with qualified production lines has been reported. Tabatt *et al.* (3) found that SLN and liposome formulated from the same cationic lipid showed equipotent *in vitro* transfection efficiencies implying that as SLN can be produced in large scale and under favorable technology parameters, they might become a competitor of the well-established repertoire of non viral transfection agents leading by cationic liposome.

The positively charged SLN would bind to polyanionic DNA via electrostatic force leading to SLN-DNA complex that will protect DNA from interaction with small molecules in environment (2) and will be taken into cell by an endocytosis process (4). Calvo *et al.* (5) reported that submicron particles could be more taken into cell by endocytosis mechanism than those of microparticles. Therefore, both size and zeta potential value are important physicochemical particle properties, as they determine the physical stability as well as the biopharmaceutical properties of the preparation (6).

In many developed countries, the morbidity and mortality associated with human immunodeficiency virus (HIV) infection have markedly declined due to the availability and use of highly active antiretroviral therapy (HAART). For some developing countries, the spread of HIV is still rampant and accepted as a public health problem. This might be because the social programs intended to reduce the spread of HIV have generally proven insufficient and many HIV patients in poor developing countries could not reach the high cost HAART. However, a long-term usage of HAART is limited by drug resistance development and severe side effects including pharmacokinetic drug interactions. Thus, the new antiretrovirals acting on alternative targets to avoid cross-resistance with old compounds and with improved systemic tolerability profiles are required (7). In addition, a safe and cost effective vaccine for the prevention of HIV infection is also urgently needed to decrease the epidemic.

Although the potential of plasmid DNA (pDNA) vaccine for eliciting antigen specific immune responses by using cationic microparticles, chitosan, and cationic liposome as carriers for pDNA delivery has been extensively studied (8), there is still a lack of data for *in vitro* SLN-pDNA delivery especially for HIV pDNA vaccine delivery. In this study, the effect of SLN formulation compositions on size and zeta potential was studied using response surface methodology, a face-centered central composite design, to depict the effect of surfactant, cationic lipid and cholesterol on size and zeta potential of SLN and to generate model equations for size and zeta potential prediction from their known composition concentrations within the experiment region. In addition, the effect of SLN formulation compositions on the potential for *in vitro* pHIS-HIV-hugag, a HIV pDNA vaccine, transfection was also evaluated.

MATERIALS AND METHODS

Materials

Cetylpalmitate (Sigma-Aldrich Inc., USA), dimethyldioctadecyl ammonium bromide (DDAB) (Sigma-Aldrich Inc., USA), cholesterol (Fluka Inc., USA), agarose (Sigma-Aldrich Inc., USA) were purchased from S. M. Chemical supplies Co., Ltd. (Bangkok, Thailand). Span 85 was kindly donated by East Asiatic (Thailand) Public Co., Ltd. (Bangkok, Thailand). Tween 80, propylene glycol, methyl paraben and propyl paraben were provided by Srichand United Dispensing Co., Ltd. (Bangkok, Thailand). Sodium hydroxide (Merck, Germany), hydrochloric acid (Merck, Germany), glacial acetic acid (Merck, Germany), tris base (Merck, Germany) and ethylenediaminetetraacetic acid (EDTA) (Sigma-Aldrich Inc., USA) were supplied by Samchai Chemical Co., Ltd. (Bangkok, Thailand). Ethidium bromide, all media and reagents for cell culture, cell transfection and western blot were purchased from Invitrogen (USA) via Gibthai Co., Ltd. (Bangkok, Thailand).

The pHIS-HIV-hugag, pDNA expressing a human multiple epitope gag protein used in this study were kindly provided from the Division of Allergy and Clinical Immunology, Faculty of Medicine, Chulalongkorn University.

SLN Production

The SLN were produced using the hot high pressure homogenization technique as described by Mehnert and Mäder (9). Briefly, cetylpalmitate was melted at about 10°C above its melting point. Then, cholesterol (for some formulations) and DDAB were added and stirred continuously until they melted completely. The mixture of molten lipid was dispersed into a hot aqueous solution containing mixture

Table I. Formulation Composition of SLN

Ingredients	Percent Content
Cetylpalmitate	3
Surfactant[a]	Varied
DDAB	Varied
Cholesterol	Varied
Propylene glycol	5
Paraben concentrate	1
Purified water to make	100

[a] A mixture of Tween 80 and Span 85 in a ratio of 7:3 (w/w)

Table II. Concentrations and Coded Level of Variables for Experimental Design

Variable	Concentration of Variable (%w/w)				
	Low Level (−)	Center Point (0)	High Level (+)	Low Level of Axial Point (−α)	High Level of Axial Point (+α)
Surfactant	2.00	5.00	8.00	2.00	8.00
DDAB	0.08	0.64	1.20	0.08	1.20
Cholesterol	0.00	0.34	0.68	0.00	0.68

of surfactants, propylene glycol and paraben concentrate and was then stirred with a high speed stirrer (Ultra Turrax, Germany) for 1 min to form a pre-emulsion system. The dispersion was homogenized by using Emulsiflex-B3 (Avestin Inc., Canada) at a pressure of 15,000 psi for 5 cycles and allowed to cool down to room temperature. The formulations of SLN studied in this experiment are shown in Table I.

Experimental Design

To depict the influence of SLN formulation on their size and zeta potential, a face-centered central composite design was selected. The advantage of this method is that adding center points and star points to the initial factorial design allow the fitting of experimental data to a quadratic model (6) and response surfaces plotting. Once the model is calculated, it can be used to predict a certain response for a known content of formulation composition. From preliminary experiments, the three factors listed; surfactant, DDAB and cholesterol were critical variables for particle size and zeta potential of the SLN fixed lipid matrix content system. The variables and their levels for the face-centered central composite experimental design are shown in Table II. The design containing 18 runs; i.e., 8 (2^3) factorial points, six star points and four center points as shown in Table III was generated and analyzed by the statistical software package Design-Expert V. 6 (StatEase Inc., USA).

Statistically significant F ratio ($\alpha < 0.05$) and adjusted determination coefficients (Adj-R^2) between 0.8–1 associated to non statistically significant lack of fit ($\alpha > 0.05$) were the criteria for validation of the model chosen, according to those previously suggested by Chacón *et al.* (10). For the regression coefficients, a significance test was performed to obtain the regression equations including only the terms with statistical significance. The effect of surfactant, DDAB and cholesterol on size and zeta potential were also presented as response surface plots generated by the software for two variables at a time.

Size, Zeta Potential Measurement and Morphology Observation

Particle size of SLN was analyzed by photon correlation spectroscopy (PCS) technique using Nanosizer (Malvern Instrument NanoZS, UK). Zeta potential was measured in purified water at pH 7.0 by using the same equipment. They were measured in three replicates and reported in a form of mean ± standard deviation (SD).

Table III. Face-centered Central Composite Experimental Design and Responses; Particle Size and Zeta Potential of SLN (mean ± SD)

Formulation	Code of (a, b, c)[a]	Percent Content (w/w)			Responses		
		Surfactant	DDAB	Cholesterol	Size (nm)	PI	Zeta Potential (mV)
SLN 1	(−,−,−)	2.00	0.08	0.00	140 ± 1	0.25 ± 0.01	39 ± 1
SLN 2	(+,−,−)	8.00	0.08	0.00	142 ± 3	0.23 ± 0.00	11 ± 0
SLN 3	(−,+,−)	2.00	1.20	0.00	160 ± 2	0.37 ± 0.00	58 ± 1
SLN 4	(+,+,−)	8.00	1.20	0.00	191 ± 2	0.27 ± 0.00	61 ± 1
SLN 5	(−,−,+)	2.00	0.08	0.68	150 ± 2	0.24 ± 0.01	37 ± 1
SLN 6	(+,−,+)	8.00	0.08	0.68	147 ± 1	0.32 ± 0.01	16 ± 1
SLN 7	(−,+,+)	2.00	1.20	0.68	136 ± 1	0.27 ± 0.00	50 ± 1
SLN 8	(+,+,+)	8.00	1.20	0.68	162 ± 2	0.29 ± 0.00	60 ± 2
SLN 9	(−α,0,0)	2.00	0.64	0.34	160 ± 2	0.27 ± 0.01	58 ± 1
SLN 10	(+α,0,0)	8.00	0.64	0.34	179 ± 1	0.24 ± 0.01	49 ± 1
SLN 11	(0,−α,0)	5.00	0.08	0.34	142 ± 1	0.32 ± 0.01	22 ± 1
SLN 12	(0,+α,0)	5.00	1.20	0.34	163 ± 1	0.36 ± 0.01	52 ± 1
SLN 13	(0,0,−α)	5.00	0.64	0.00	161 ± 1	0.25 ± 0.01	56 ± 1
SLN 14	(0,0,+α)	5.00	0.64	0.68	154 ± 2	0.24 ± 0.00	54 ± 1
SLN 15	(0,0,0)	5.00	0.64	0.34	166 ± 1	0.24 ± 0.00	50 ± 1
SLN 16	(0,0,0)	5.00	0.64	0.34	170 ± 3	0.25 ± 0.00	51 ± 1
SLN 17	(0,0,0)	5.00	0.64	0.34	163 ± 2	0.26 ± 0.00	51 ± 1
SLN 18	(0,0,0)	5.00	0.64	0.34	169 ± 1	0.26 ± 0.01	51 ± 1

[a] a, b, c are surfactant, DDAB and cholesterol, respectively

The morphological characteristics of SLN and SLN-pDNA complex were examined using a negative stain transmission electron microscopy (TEM) technique. Briefly, one drop of diluted sample was placed on a copper grid coated with carbon film, then stained with 0.5% w/v uranyl acetate solution and allowed to dry under room temperature. The grids were imaged using a JEM-1220 (Japan) transmission electron microscope.

Ability of SLN to Form Complex with pHIS-HIV-Hugag

The ability of SLN to form complex with polyanionic pDNA was studied by analysis of the electrophoretic mobility of pDNA within an agarose gel so-called electrophoretic mobility shift assay. In this study, the influence of formulation composition on the ability of SLN to form complex with pHIS-HIV-hugag was evaluated by comparing SLN formulations as listed; 1) effect of surfactant concentrations i.e. SLN 9, SLN 10 and SLN 15, 2) effect of DDAB concentrations i.e. SLN 11, SLN 12 and SLN 15, 3) effect of cholesterol concentrations i.e. SLN 13, SLN 14 and SLN 15.

SLN were diluted with purified water and mixed with pDNA suspension at the ratio of SLN:pDNA (weight by weight) 10,000:1, 5,000:1, 1,000:1, 500:1, 100:1 in microfuge tubes. The mixtures were allowed to form complex for 30 min at room temperature and were then loaded into 0.8% w/v agarose gels immersed in tris-acetate EDTA (TAE) running buffer to run electrophoresis for 90 min with electricity of 5 V/cm. The gels were taken to stain with 0.7%w/v ethidium bromide solution and destained with purified water after electrophoresis was finished. The fraction of mobile pDNA was observed under UV light. Images were obtained using a Geldoc documentation system (Biorad, USA).

Cell Culture

HeLa cells, human epithelial cervix carcinoma cell lines, were maintained in Dulbecco's modified eagle's medium (DMEM) supplemented with 10% fetal bovine serum (FBS). They were incubated at 37°C with 5% CO_2 atmosphere and subcultured every 3–4 days using trypsin-EDTA solution.

Cytotoxicity Assay

The cytotoxicity of SLN was determined using the alamar blue bioassay. The oxidized indigo blue form of this chromogenic indicator dye is reduced by cellular dehydrogenases, specifically targeting the mitochondrial electron transport chain, to a reduced pink form (11). The bioassay was performed according to the manufacturer's instruction. Briefly, HeLa cells were seeded on 96-well plates with a density of 10,000–20,000 cells per well and allowed to adhere overnight. SLN which were able to immobilize pDNA at the lowest ratio of SLN:pDNA were diluted in DMEM without FBS at the final concentrations of 10,000, 5,000, 1,000, 500, 400, 300, 200, 100 μg/ml.

The HeLa cell monolayers, 60–70% confluent, were washed once with phosphate buffer saline (PBS) and incubated with 200 μl of test suspensions for 24 h at 37°C. The cells were washed again with PBS and incubated with 200 μl of alamar blue solution (5% v/v in DMEM without FBS) for 24 h at 37°C. Fluorescence was read after 24–h using a Perkin–Elmer BioAssay reader (USA) set at wavelengths of 544 nm for excitation and 620 nm for emission. Wells containing medium and alamar blue without HeLa cells were used as blanks. The 100% cell viability was calculated from the results of wells containing HeLa cells with no addition of SLN. The assay was performed in 5-replicate and reported as mean % cell viability ± SD.

Transfection Study

HeLa cells were seeded on six-well plate at a density of 2×10^5–3×10^5 cells per well and allowed to adhere overnight. The medium was removed from the 70% confluent monolayer, and then cells were rinsed with PBS. The 30 μl of SLN-pDNA complex was mixed with 1,970 μl of DMEM (no FBS supplement) and added to cells. The cells were incubated with the complex for 24 h at 37°C under 5% CO_2. They were then washed once with PBS and allowed to grow for further 24 h in DMEM containing 10% FBS at 37°C under 5% CO_2. Fugene 6, a commercial non-viral transfection vector, was chosen to compare with SLN. The pHIS-HIV-hugag transfection in HeLA cells using Fugene 6 was performed at a ratio of Fugene 6: pDNA (volume by weight) 3:1 according to manufacturer's instruction (Roche Applied Science, USA).

Cells were washed twice with cold PBS and harvested using a cell scraper. They were collected by centrifugation at 10,000 rpm, 4°C for 5 min. Lysis buffer was added to cells and let them be lysed for 45 min on ice. Cell debris was spun down at 13,000 rpm, 4°C for 5 min to collect supernatant into a new tube. NuPage LDS sample buffer and NuPage reducing agent were added to the supernatant in a volume of 5 and 2 μl, respectively. The mixture was heated at 70°C for 10 min and then loaded into NuPage Novex Bis-Tris gel immersing in SDS running buffer to run electrophoresis using 200 V for 50 min.

Gag protein expressed in HeLa cells was detected by western blot technique as described in the following, the gel used in electrophoresis experiment was taken to immerse in NuPage transfer buffer for 10 min to equilibrate. Two filter papers and a transfer membrane were also soaked in NuPage transfer buffer for 1 min. Then, a soaked filter paper was placed on bottom platinum anode of a blot module (Biorad, USA) followed by the soaked transfer membrane, the equilibrated gel and remaining soaked filter paper, respectively. A stainless steel cathode and safety cover were placed on. The experiment was performed using 10 V for 30 min After that, the transfer membrane was taken to wash with PBS and blocked with 10% v/v non fat milk (Skim milk, USA) in PBS for 1 h. It was then washed with PBS three times and incubated in 183-H12-5C Monoclonal antibody (NIH AIDS research and reference reagent, USA) overnight. The membrane was washed, blocked and washed using the same reagents. Then, it was incubated in Anti-Mouse Immunoglobulins (DakoCytomation, Denmark) for 4 h. The membrane was washed, blocked and washed again, and then incubated in substrate solution containing BCIP (x-phosphate/5-bromo-4-chloro-3-indolyl-phosphate) and NBT (4-nitro blue tetrazolium-chloride) (Boehringer Mannheim, USA). The dark blue band will appear in a lane containing gag protein.

RESULTS AND DISCUSSION

Characterization of SLN

The SLN produced according to the generated experiment design possessed diameter in a nanometer range with positive surface charges due to the ionization of an amine group in DDAB molecule. The average particle size, polydispersity index (PI) and zeta potential shown in Table III suggested that a fine control of particle size and zeta potential of SLN could be achieved by combination of the three variables; surfactant, DDAB and cholesterol concentration. TEM micrograph shown in Fig. 1a of SLN 15 as a representative of all formulation presented a spherical shape of SLN.

Experimental Design

The regression analysis of the results generated the following polynomial equations which the model F ratios were statistically significant at $\alpha < 0.05$ with Adj-R^2 value in the range of 0.8–1 and were non statistically significant lack of fit at $\alpha > 0.05$.

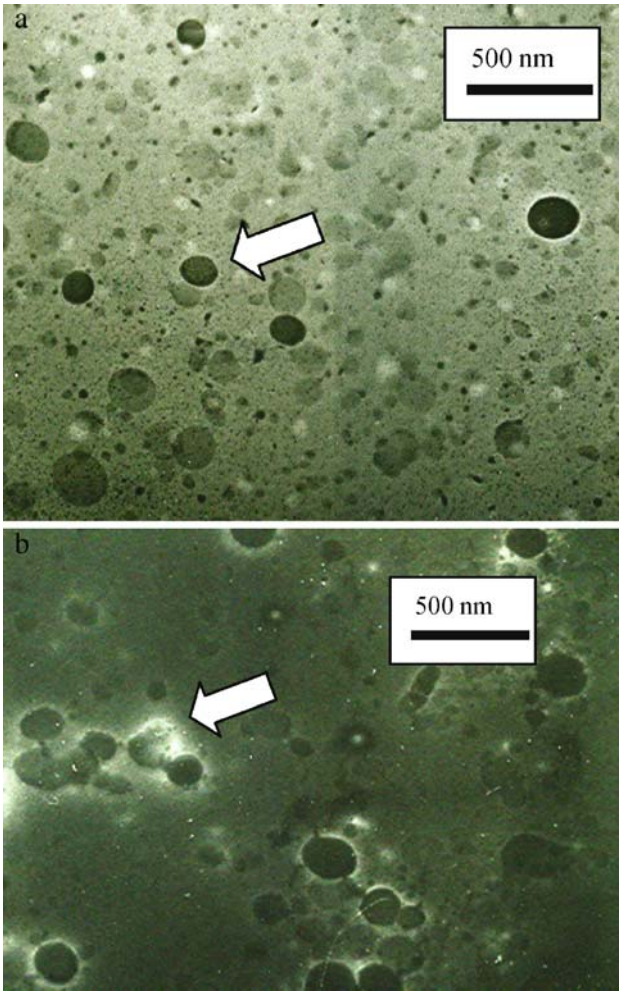

Fig. 1. Negative stain transmission electron micrograph of SLN 15 (**a**) and SLN 15-pDNA complex (**b**).

Table IV. Results of Statistical Analysis of the Experimental Design

Responses	Sources		
	Model p Value	Adj-R^2	Lack of Fit Test p Value
Particle size	<0.0001	0.9502	0.5470
Zeta potential	<0.0001	0.9982	0.4125

$$\text{Particle size} = 144.36 - 6.17a + 58.03b + 51.28c + 0.60a^2 - 37.23b^2 - 53.64c^2 + 4.18ab - 44.22bc \quad (1)$$

$$\text{Zeta potential} = 46.93 - 7.07a + 67.40b - 25.85c + 0.20a^2 - 46.93b^2 + 27.88c^2 + 4.64ab + 1.90ac - 7.79bc \quad (2)$$

Where a, b, c are concentrations of surfactant, DDAB and cholesterol, respectively. The statistical analysis results shown in Table IV suggested that there was less than 0.01% chance that the model F value of model Eqs. (1) and (2) occurred due to noise. Their Adj-R^2 showed that the model Eq. (1) could explain 95.02% of the variability and also the model Eq. (2) could explain 99.82%. The p values of the lack of fit test of the two models were not significant. This pointed out that these model equations fitted the data well. Therefore, the two quadratic models could describe adequately the data and could be used to navigate the design space. However, the model equations containing significant interaction terms of the three variables suggested that the main effect of each variable on particle size and zeta potential of SLN was interfered by the effect of another variable. The three-dimensional response surfaces and contours shown in Figs. 2, 3 and 4 were plotted on the basis of the model equations to depict the effect of model variables i.e. surfactant, DDAB and cholesterol concentration on particle size and zeta potential.

The model verification results are shown in Table V and compared to observed value suggesting that these model equations could be used to predict size and zeta potential of SLN.

Effect of Formulation Compositions on Particle Size and Zeta Potential

Effect of Surfactant and DDAB on Particle Size and Zeta Potential of SLN

At the high level of DDAB in Fig. 2a, the increment of surfactant content markedly increased the particle size of SLN. This was probably that DDAB, an amphiphilic compound, could be adsorbed and located more at the interface between oil droplet and water phase as the surfactant content increased. This phenomenon also led to higher zeta potential of SLN as shown in the effect of surfactant and DDAB on zeta potential of SLN. Therefore, the obtained nanoparticles would be larger and possessed

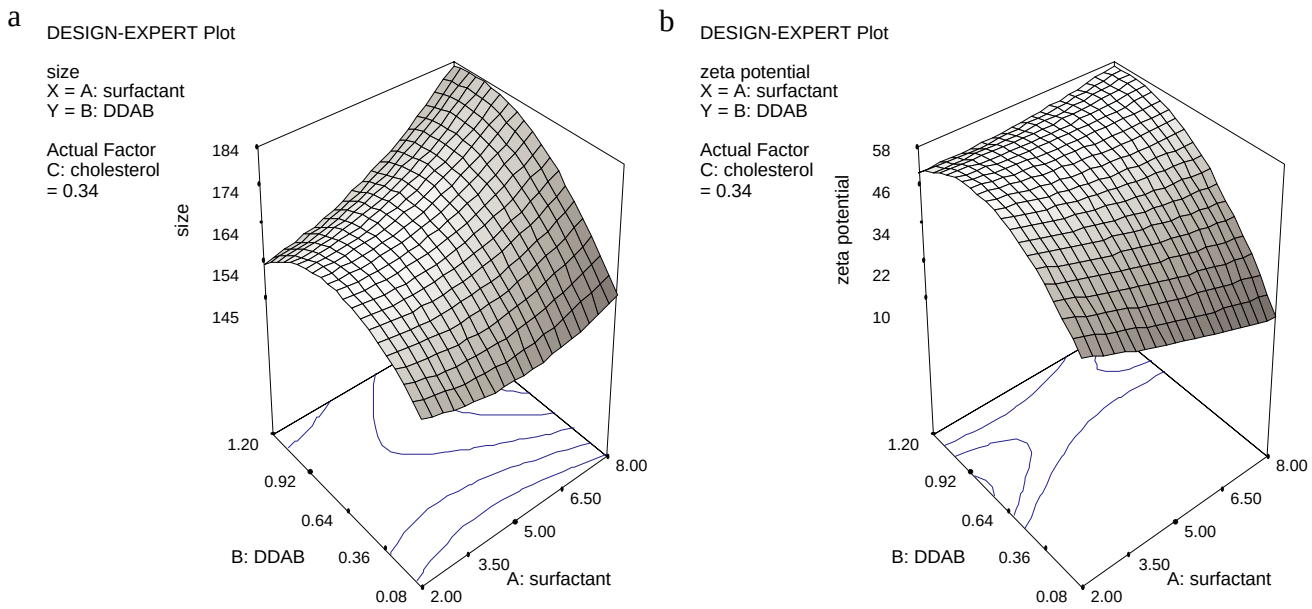

Fig. 2. Response surface for size (**a**) and zeta potential (**b**) of SLN: effect of surfactant and DDAB.

more positive surface charge. Moreover, the excess surfactant accumulating at the SLN surface also increased the particle size of SLN similarly to a previous study indicating the effect of phospholipids content on size and zeta potential of glyceryl tripalmitate SLN (12). At the lower level of DDAB, the size of SLN slightly decreased with the increase in surfactant content to about 5%. This might be a consequence of lower interfacial tension between oil phase and water phase by surface active agents resulted in increment of surface curvature of smaller oil droplets (13). However, at surfactant content above 5%, the size of SLN was increased which could be attributed to the accumulation of excess surfactant molecules at nanoparticle surface.

The effect of surfactant and DDAB on zeta potential of SLN depicted in Fig. 2b shows that the increment of surfactant content at the high level of DDAB gradually increased the zeta potential of SLN from 50 to 58 mV. This was probably due to DDAB molecules could be adsorbed and located more at the interface of oil droplet as surfactant content increased. At the lower level of DDAB, the increased surfactant content markedly reduced the positive surface charge due to the head group of DDAB at interface might be shielded by the head group of surfactant adsorbed at interface and also the surfactant molecules accumulating around the SLN surface.

Effect of Surfactant and Cholesterol on Particle Size and Zeta Potential of SLN

As seen in Fig. 3a, the size of SLN with and without cholesterol increased in the same manner with the increment

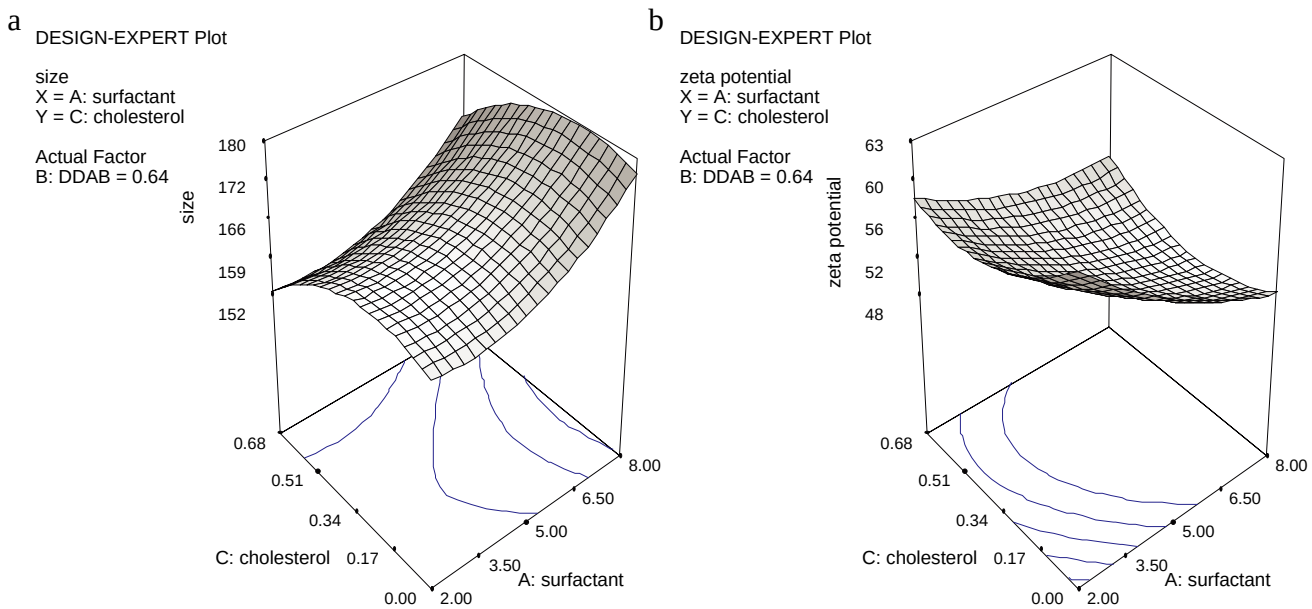

Fig. 3. Response surface for size (**a**) and zeta potential (**b**) of SLN: effect of surfactant and cholesterol.

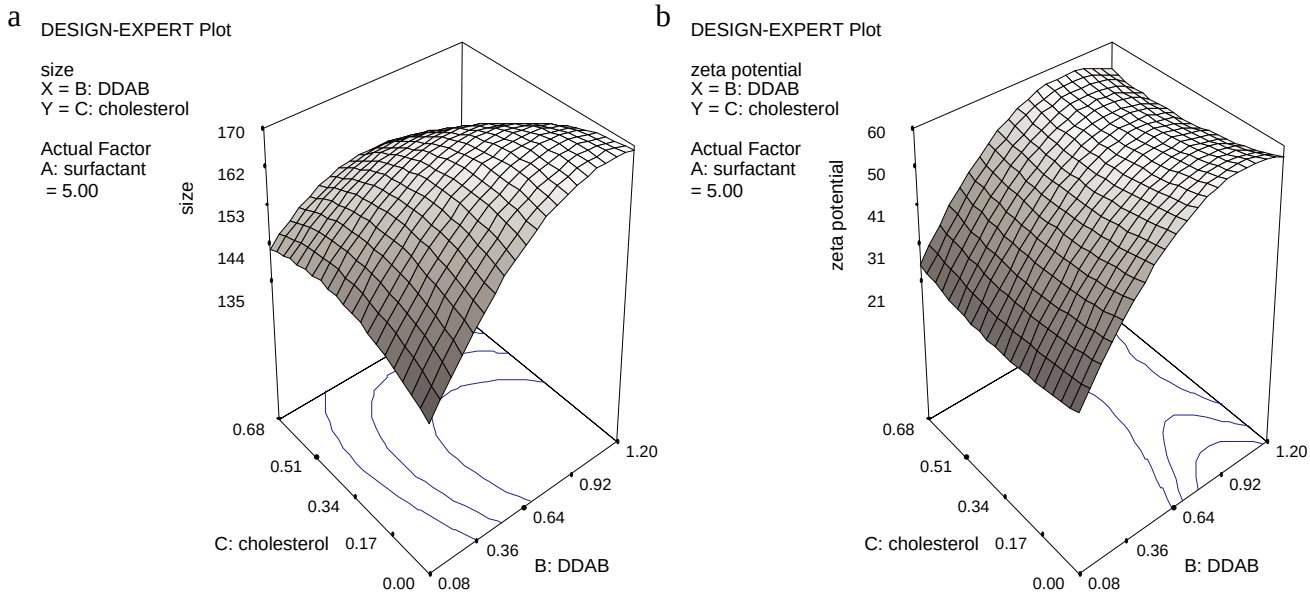

Fig. 4. Response surface for size (**a**) and zeta potential (**b**) of SLN: effect of DDAB and cholesterol.

of surfactant content. This showed that the main effect of cholesterol did not affect the main effect of surfactant on the size of SLN. However, it was found that the SLN containing high level of cholesterol tended to possess smaller particle size than those of the SLN without cholesterol. This result was in accordance with previous study by Jain *et al.* (14) showing that the high ratio of cholesterol/lipid matrix reduced the SLN diameter. It might be that the cholesterol incorporated in SLN interacted with surface active molecules at the interface of oil droplets. This led to a rigid surfactant layer including decrement in van der Waal attraction and promotion of net repulsion forces between oil droplets therefore, agglomeration and coalescence of small oil droplets were reduced. This phenomenon was also found in liposome system consisting of phospholipids and cholesterol (15). In addition, the interaction between cholesterol and surface active agent might increase in surface curvature of oil droplet and leading to small size of SLN after cooling down.

It can be seen in Fig. 3b that by increasing the surfactant content the zeta potential of all nanoparticles were reduced. This could be explained by the adsorption and the accumulation of surfactant molecules on the surface of nanoparticle. At the surfactant concentration of less than 6.5%, SLN without cholesterol had more positive surface charge than SLN containing cholesterol. It was possible that the presence of cholesterol might limit DDAB lipophilic chain partitioning into lipid core, thus the number of DDAB molecules adsorbed at interface were reduced. Nevertheless, at the concentration of surfactant higher than 6.5%, SLN with cholesterol possessed higher zeta potential. This might be due to the effect of cholesterol on the arrangement of surfactant molecules and DDAB molecules at the interface of oil droplet. Therefore, the head group of DDAB was less shielded by the head group of surfactant and surfactant molecules. However, it was found that the difference between maximum and minimum zeta potential value of SLN in Fig. 3b was only 15 mV. This implied that within the experiment region, the magnitude of interaction effect between surfactant and cholesterol on zeta potential of SLN was small as seen in the small value of ac regression coefficient in model Eq. (2).

Effect of DDAB and Cholesterol on Particle Size and Zeta Potential of SLN

The size of SLN containing high level of cholesterol increased with the increment of DDAB content to 0.64% as shown in Fig. 4a. This was possible that more DDAB molecules adsorbed at the interface between oil phase and water phase, thus resulting in particle size increment. However, the increase in DDAB content more than 0.64% led to a reduction of particle size of SLN to close to the system containing low content of DDAB. As previously discussed, it might be that cholesterol markedly affected the

Table V. Comparison of Observed Values and Predicted Value of Responses

Factors			Observed Value		Predicted Value		
Surfactant (g)	DDAB (g)	Cholesterol (g)	Size (nm)	Zeta Potential (mV)	Size (nm)	Zeta Potential (mV)	*p* Value
5.00	0.24	0.34	156 ± 2	33 ± 1	153	33	<0.05
5.00	0.08	0.34	140 ± 2	22 ± 1	145	21	<0.05
5.00	0.16	0.00	145 ± 2	29 ± 1	140	30	<0.05
5.00	0.16	0.68	151 ± 2	31 ± 1	145	31	<0.05

Table VI. SLN:pDNA Immobilized Ratio (w/w)

Formulation	SLN:pDNA Immobilized Ratio
SLN 9	5,000:1
SLN 10	10,000:1
SLN 11	cd[a]
SLN 12	5,000:1
SLN 13	1,000:1
SLN 14	1,000:1
SLN 15	1,000:1

[a] could not determine

arrangement of the increased DDAB molecules at the interface of oil droplets resulting in smaller SLN. This result was confirmed by the continuous increment of particle size of SLN without cholesterol as DDAB content increased.

Figure 4b suggests that the increment of DDAB concentration markedly increased the zeta potential of both with and without cholesterol SLN systems. This was a result of the rise in charge density of adsorption layer upon the increase in DDAB molecules at interface which was consistent with the effect of dodecyl pyridinium chloride on zeta potential of oil-in-water emulsion system studied by Goluob *et al.* (13). Further increase of DDAB concentration gradually increased the zeta potential to reach its maximum value at DDAB concentration of 0.92% and finally, it tended to be stable. This suggested that the saturation of cationic lipid adsorption occurred when the zeta potential reached a maximum and the surface of SLN was completely covered with DDAB molecules. Gu *et al.* (16) and Ahlin *et al.* (17) also demonstrated a similar saturation plot pattern for zeta potential of silicone-oil-in-water emulsion droplets versus concentration of cetyltrimethylammonuim bromide (CTAB) and glyceryl tripalmitate SLN versus phospholipid content, respectively.

Ability of SLN to Form Complex with pDNA

SLN 9 to SLN 15 used in this study were able to immobilse pDNA in a supplied electric field at the varying SLN:pDNA ratios by forming SLN-pDNA complexes (Fig. 1b) except for SLN 11 as shown in Table VI. This was explained that the addition of cationic lipid into SLN provided a multivalent positive surface charge that could interact via electrostatic with the negative charge on the pDNA phosphate backbone (18). Because the ability of nanoparticle to form complex with pDNA depended on positive surface charge of nanoparticle (19), SLN 11 possessing the lowest zeta potential could not bind to pDNA at any ratios. According to statistical analysis of zeta potential by one-way ANOVA with Tukey's multiple comparison at p value of less than 0.05, the SLN containing different surfactant contents; SLN 10 and SLN 15 possessed a comparable zeta potential but their ability to form complex with pDNA were not equivalent. It was found that SLN 15 consisting lower surfactant content began to form complex with pDNA at the SLN:pDNA ratio = 1,000:1 while SLN 10 was able to immobilize pDNA at 10,000:1. This was probably that the more excess surfactant molecules accumulating on SLN 10 surface led to the weak electrostatic interaction between surface of SLN and pDNA that could not immobilize pDNA in the electric field at the lower ratio of SLN:pDNA. Although the SLN 15 contained more surfactant content and possessed less zeta potential than that of SLN 9, its ability to form complex with pDNA was greater. This result showed that the optimum surfactant content on SLN surface played an importance role on pDNA interaction. Moreover, it might cause any additional interaction between SLN surface and pDNA apart from the electrical interaction such as hydrophobic force between the surfactant adsorbed on surface of SLN and pDNA (18).

Due to insufficient positively charges of SLN 11 with the lowest DDAB content, it could not form complex with pDNA at any ratios. Surprisingly, although SLN 12 possessed a comparable zeta potential to that of SLN 15, it could retain pDNA in the electric field at higher ratio of SLN:pDNA. This might be the excess DDAB covering the SLN 12 surface led to the reduction of interaction between the surface of SLN and pDNA. Therefore, the pDNA was easily detached by the electrical force.

SLN 13, SLN 14 and SLN 15 containing varying cholesterol contents formed complex with pDNA at the same ratio of SLN:pDNA = 1,000:1. There was no doubt about the ability of SLN 13 and SLN 14 exhibiting comparable zeta potential. But SLN 15 containing medium cholesterol level and possessing a significantly lower zeta potential than that of SLN 13 could immobilize pDNA at the same ratio. The result here confirmed that not only the electrical force affected the ability of SLN to form complex with pDNA but also the additional interaction between surface of SLN and pDNA. Therefore, SLN 13, SLN 14 and SLN 15 were selected to further study due to their lowest immobilized ratio of SLN:pDNA.

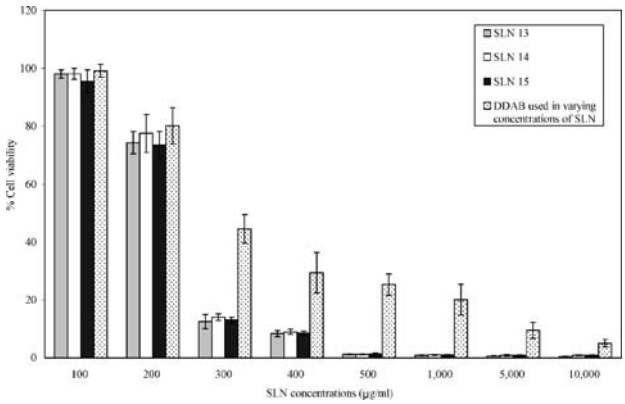

Fig. 5. Percent cell viability of HeLa cells incubated in varying concentrations of SLN and DDAB for 24 h.

Cytotoxicity Assay

In vitro cytotoxicity assay was performed in HeLa cells by determining the ability of cells to reduce the oxidised blue

Fig. 6. Gag protein in cell lysates from HeLa cells incubated with Fugene 6-pHIS-HIV-hugag complex and SLN-pHIS-HIV-hugag complexes for 24 h detected by western blot technique; Fugene 6 (*lane 1*), SLN 14 (*lane 2*), SLN 15 (*lane 3*), SLN 13 (*lane 4*), naked pHIS-HIV-hugag (*lane 5*),: SLN 14 incubated for 4 h (lane 6) and marker (*lane 7*).

form of chromogenic indicator to be a reduced pink form. The viability of HeLa cells after incubation with varying concentrations of SLN in DMEM without FBS for 24 h is shown in Fig. 5.

The results showed that high concentrations of SLN 13, SLN 14 and SLN 15 were very toxic to cells that only 0.1–15% of HeLa cells still survived in a range of 300–10,000 μg/ml of SLN in DMEM. However, most of them were viable in 100–200 μg/ml of SLN in DMEM. This might be the toxicity of a cationic lipid, DDAB, synergisted with other formulation compositions as seen in the results of cytotoxicity test of DDAB used in varying concentrations of SLN 13, SLN 14 and SLN 15 (Fig. 5) in HeLa cells. Tabatt *et al.* (4) demonstrated that SLN containing DDAB was more toxic to COS-1 cells than SLN containing EQ1 or DOTAP but less toxic than SLN made from CPC or CTAB. This might be that the ester bonds in EQ1 and DOTAP molecule allowed them to be metabolized easily in mammalian cells while DDAB containing two aliphatic chains directly linking to amine group was hardly transformed. By the proper selection of DDAB concentrations, the successful transfection was demonstrated in COS-1 cells using ß-galactosidase pDNA.

Transfection Study

This experiment was performed to study the effect of SLN formulation compositions on potential for *in vitro* pHIS-HIV-hugag transfection. Therefore, the high selectivity technique for specific protein detection used in the previous work (20), the western blot technique, was selected to detect the gag protein expressed in HeLa cells.

The transfection study was performed by using SLN at the concentration of 200 μg/ml that would form complex with 0.4 μg pDNA at the ratio of SLN:pDNA = 1,000:1 in 2.0 ml of incubation medium. It was found that a very low intensity of gag protein band could be obtained in cell lysates from HeLa cells incubated with SLN 14-pDNA complexes for 4 h as seen in Fig. 6 (lane 6) while lysates from cells incubated with SLN 13- or SLN 15-pDNA complexes or naked pDNA could not detected the gag protein (data not shown).

The intensity of gag protein band in Fig. 6 were more intense when HeLa cells were incubated with SLN-pDNA complexes up to 24 h. Nevertheless, the gag protein could not be observed from cells incubated with naked pDNA (lane 5). This showed that HeLa cells could be transfected with pHIS-HIV-hugag by using these cationic SLN. Furthermore, it was visually observed that HeLa cells incubated with SLN 14-pDNA complexes (lane 2) expressed more gag protein than those of cells incubated with SLN 15-pDNA complexes (lane 3) or SLN 13-pDNA (lane 4) or naked pDNA. The results here suggested that the SLN containing high cholesterol content could increase gag protein expression in HeLa cells. This might be the activity of cholesterol which is usually used as a helper lipid in cationic liposomes (21–23). In addition, the smallest complex size of SLN 14-pDNA (322 ± 2 nm) would be taken into cell by endocytosis easier than those of larger SLN-pDNA complex; SLN 13-pDNA (375 ± 3 nm) and SLN 15-pDNA (352 ± 1 nm) (18).

However, when the transfection potential of SLN was compared to the established transfection agent used in the previous work (20), Fugene 6 (lane 1), it was ranked only low to moderate level. This suggested that although the obtained SLN had ability to use as a transfection vector, their composition should be reformulated to improve its potential for *in vitro* transfection.

CONCLUSIONS

The influence of surfactant, DDAB and cholesterol concentrations on size and zeta potential of SLN could be described by the quadratic model equations and their surface responses. The statistically significant interaction terms in the model equations suggested the main effect of these factors was involved by each other. It was found that within the experiment region, the increment of surfactant content in SLN tended to increase size and reduce zeta potential. In addition, size and zeta potential considerably increased with increment of DDAB content. The addition of cholesterol in SLN tended to led to size and zeta potential reduction. The ability of SLN to form complex with pHIS-HIV-hugag was not only affected by an electrical force but also the interaction between surface of SLN and pHIS-HIV-hugag. The SLN containing medium content of surfactant (5%), DDAB (0.64%) and with or without cholesterol could immobilize the pHIS-HIV-hugag under a supplied electric field at the lowest SLN:pDNA ratio, 1,000:1. The SLN cytotoxicity test showed that HeLa cells could tolerate in a range of 100 to 200 μg/ml of SLN in DMEM without FBS. The results of transfection study at the concentration of 200 μg/ml of SLN showed the potential of SLN for using as an *in vitro* pHIS-HIV-hugag transfection vector, particulary the SLN containing high content of cholesterol (0.68%) with medium content of surfactant (5%) and DDAB (0.64%). This finding suggested that the optimum SLN formulation could promote the transfection efficiency of pHIS-HIV-hugag in HeLa cells. However, the ability of obtained SLN to use as a transfection vector was lower than the established transfection reagent. Thus, improvement in SLN formulation such as using powerful helper lipid, low toxic cationic lipid possessing high potential for transfection and coating cell specific ligand on nanoparticle surface should be further investigated.

ACKNOWLEDGMENTS

The authors gratefully acknowledge the support for this work by the Thailand Research Fund (TRF) under the Royal Golden Jubilee PhD program grant and the Rachadapisek Sompoch Fund, Graduate School, Chulalongkorn University for providing Chulalongkorn University 90th Anniversary grant.

REFERENCES

1. M. J. Alonso. Nanomedicines for overcoming biological barriers. *Biomed. Pharmacother.* **58**:168–172 (2004).
2. C. Olbrich, U. Bakowsky, C. Lehr, R. H. Müller, and C. Kneuer. Cationic solid-lipid nanoparticles can efficiently bind and transfect plasmid DNA. *J. Control Release* **77**:345–355 (2001).
3. K. Tabatt, C. Kneuer, M. Sameti, C. Olbrich, R. H. Müller, C.

Lehr, and U. Bakowsky. Transfection with different colloidal systems: comparison of solid lipid nanoparticles and liposomes. *J. Control Release* **97**:321–332 (2004).
4. K. Tabatt, M. Sameti, C. Olbrich, R. H. Müller, and C. Lehr. Effect of cationic lipid and matrix lipid composition on solid lipid nanoparticles-mediated gene transfer. *Eur. J. Pharm. Biopharm.* **57**:155–162 (2004).
5. P. Calvo, M. J. Alonso, J. L. Vila-Jato, and J. R. Robinson. Improved ocular bioavailability of indomethacin by novel ocular drug carriers. *J. Pharm. Pharmacol.* **48**:1147–1152 (1996).
6. J. Vandervoort and A. Ludwig. Biocompatible stabilizers in the preparation of PLGA nanoparticles: a factorial design study. *Int. J. Pharm.* **238**:77–92 (2002).
7. S. Sierra, B. Kupfer, and R. Kaiser. Basics of the virology of HIV-1 and its replication. *J. Clin. Virol.* **34**:233–244 (2005).
8. C. P. Locher, D. Putnam, R. Langer, S. A. Witt, B. B. Ashlock, and J. A. Levy. Enhancement of a human immunodeficiency virus env DNA vaccine using a novel polycationic nanoparticle formulation. *Immunol. Lett.* **90**:67–70 (2003).
9. W. Mehnert and K. Mäder. Solid lipid nanoparticles production, characterization and applications. *Adv. Drug Deliv. Rev*. **47**: 165–196 (2001).
10. M. Chacón, L. Berges, J. Molpeceres, M. R. Aberturas, and M. Guzman. Optimized preparation of poly D,L (lactic-glycolic) microspheres and nanoparticles for oral administration. *Int. J. Pharm.* **141**:81–91 (1996).
11. M. Davoren, S. N. Shúilleabháin, M. G. J. Hartl, D. Sheehan, N. M. O'Brien, J. O'Halloran, F. N. A. M. V. Pelt, and C. Mothersill. Assessing the potential of fish cell lines as tools for the cytotoxicity testing of estuarine sediment aqueous elutriates. *Toxicol. In Vitro* **19**:421–431 (2005).
12. M. A. Schubert and C. C. Müller-Goymann. Characterisation of surface-modified solid lipid nanoparticles (SLN): influence of lecithin and nonionic emulsifier. *Eur. J. Pharm. Biopharm.* **61**:77–86 (2005).
13. T. P. Goloub and R. J. Pugh. The role of the surfactant head group in the emulsification process: binary (nonionic-ionic) surfactant mixtures. *J. Colloid Interface Sci.* **291**:256–262 (2005).
14. S. K. Jain, M. K. Chourasia, R. Masuriha, V. Soni, A. Jain, N. K. Jain, and Y. Gupta. Solid lipid nanoparticles bearing flurbiprofen for transdermal delivery. *Drug Deliv.* **12**:207–215 (2005).
15. E. F. de Souza and O. Teschke. Liposome stability verification by atomic force microscopy. *Rev. Adv. Mater. Sci.* **5**:34–40 (2003).
16. Y. Gu and D. Li. The ζ-potential of silicone oil droplets dispersed in aqueous solutions. *J. Colloid Interface Sci.* **206**:346–349 (1998).
17. P. Ahlin, J. Kristl, and J. Smid-Korbar. Optimization of procedure parameters and physical stability of solid lipid nanoparticles in dispersions. *Acta Pharm.* **48**:259–267 (1998).
18. S. Pang, H. Park, Y. Jang, W. Kim, and J. Kim. Effects of charge density and particle size of poly(styrene/(dimethylamino)ethyl emthacrylate) nanoparticle for gene delivery in 293 cells. *Colloids Surf., B Biointerfaces* **26**:213–222 (2002).
19. A. Roland and S. M. Sullivan. *Pharmaceutical gene delivery systems*, Marcel Dekker, USA, 2003.
20. M. A. Egan, S. Megati, V. Roopand, D. Garcia-Hand, A. Luckay, S. Chong, M. Rosati, S. Sackitey, D. B. Weiner, B. K. Felber, G. N. Pavlagis, Z. R. Israel, J. H. Eldridge, and M. K. Sidhu. Rational design of plasmid DNA vaccine capable of eliciting cell-mediated immune responses to multiple HIV antigen in mice. *Vaccine* **24**:4510–4523 (2006).
21. Z. Cui and R. J. Mumper. Topical immunization using nano-engineered genetic vaccines. *J. Control Release* **81**:173–184 (2002).
22. C. M. Wiethoff, J. G. Smith, G. S. Koe, and C. R. Middaugh. The potential role of proteoglycans in cationic lipid-mediated gene delivery: studies of the interaction of cationic lipid-DNA complexes with model glycosaminoglycans. *J. Biol. Chem.* **276**:32806–32813 (2001).
23. C. Hung, T. Hwang, C. Chang, and J. Fang. Physicochemical characterization and gene transfection efficiency of lipid emulsions with various co-emulsifiers. *Int. J. Pharm.* **289**:197–208 (2005).